POLITECNICO
MILANO 1863

DIPARTIMENTO DI MECCANICA

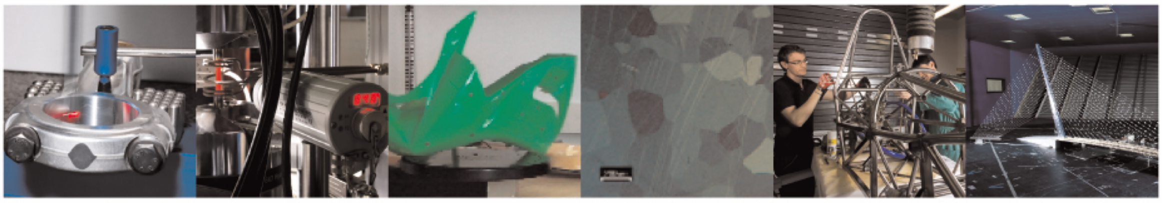

Analysis of the Spb method for geometries where ηpl depends on a/W

Egon Rolf Delgado Ramírez, Juan Elias Perez Ipiña, Enrique Mariano Castrodeza

This is a post-peer-review, pre-copyedit version of an article published in Engineering Fracture Mechanics. The final authenticated version is available online at:
http://dx.doi.org/j.engfracmech.2020.107416

DIPARTIMENTO DI MECCANICA ■ POLITECNICO DI MILANO
via G. La Masa, 1 ■ 20156 Milano ■ EMAIL (PEC): pecmecc@cert.polimi.it
http://www.mecc.polimi.it
Rev. 0

Analysis of the S_{pb} method for geometries where η_{pl} depends on *a/W*

Egon Rolf Delgado Ramírez[a]*, Juan Elias Perez Ipiña[ab], Enrique Mariano Castrodeza[ac]

[a]*Laboratory of Fracture Mechanics, COPPE/Federal University of Rio de Janeiro, P.O. Box 68505, 21941-972 Rio de Janeiro, Brazil*

[b]*Fracture Mechanics Group, CONICET, Q8300IBX Neuquén, Argentina*

[c]*Department of Mechanical Engineering, Polytechnic of Milan, Via La Masa 1, 20156 Milan, Italy*

Abstract

Since its proposal, the simplified S_{pb} method has been successfully applied to the fracture toughness evaluation of metallic and polymer materials. However, some points of this methodology remain unclear, like the applicability on standardized geometries in which η_{pl} depends on the *a/W* ratio. In order to discuss this and other aspects, theoretical analyses of the S_{pb} method were made and some experimental tests were performed. The theoretical analysis revealed that considerable differences in C(T) and SE(T) geometries could be present when the same η_{pl} factor for both blunt notched and pre-cracked specimens is used. To minimize these differences, the use of the most general expression of the S_{pb} method in addition to η_{pl} factors provided by the standards for geometries where η_{pl} change with *a/W* is proposed. The proposed experimental methodology, based on the load separation and on η_{pl} factors provided by the standards, proved to be suitable for C(T) geometry, whereas for SE(T) geometry the results indicate that more research is still needed.

Keywords: Load separation method; *a/W* ratio; theoretical S_{pb} curves; C(T) geometry; SE(T) geometry.

*Corresponding author: egon@metalmat.ufrj.br

Nomenclature

a	crack length
a_0	initial crack length of pre-cracked specimens
a_b	notch length of blunt notched specimens
a_f	final crack length of pre-cracked specimens
a_p	crack length of pre-cracked specimens
a_i	i-th crack extension prediction of pre-cracked specimens
b_0	initial remaining ligament of pre-cracked specimens
b_b	remaining ligament length of blunt notched specimens
b_p	remaining ligament length of pre-cracked specimens
B	specimen thickness
$G(a/W)$	geometry function
$H(v_{pl}/W)$	deformation function
m	power law exponent
P	applied load
P_b	applied load on blunt-notch specimens
P_p	applied load on pre-cracked specimens
W	specimen width
S_{ij}	separability parameter of blunt notched specimens
S_{pb}	separability parameter of a pre-cracked and blunt notched specimens
Δa	crack extension
Δa_p	physical crack extension
$\Delta a_{predicted}$	predicted crack extension
v_{pl}	plastic displacement
η_{pl}	eta plastic factor

η_{plCMOD} eta plastic factor derived from CMOD

σ_{UTS} ultimate tensile strength

σ_Y effective yield strength

BN blunt notch specimen

C(T) compact specimen

CMOD crack mouth opening displacement

$CMOD_{pl}$ plastic component of crack mouth opening displacement

SE(B) single edge bend specimen

SE(T) single edge tension specimen

LLD load line displacement

LLD_{pl} plastic component of the load line displacement

PC pre-cracked specimen

UC unloading compliance

1 Introduction

The S_{pb} method can be used to estimate of stable crack growth in fracture mechanic tests. Although there are also other well-established techniques for this purpose as unloading compliance, load normalization, electric potential drop, among others, S_{pb} presents advantages in some situations. Normalization techniques require a reasonable level of data processing, while unloading compliance and electrical potential drop techniques need specific instrumentation and data acquisition equipment. In cases where specific instrumentation is not available or fracture extensometers are not suitable (*i.e.* high temperature testing, corrosive environments, etc.), the application of S_{pb} method could be considered because only two monotonic tests of the same material in the same geometry are necessary (one of them on a pre-cracked specimen (PC) and the another on a blunt notched specimen (BN)).

The S_{pb} methodology is based on the load separation theory proposed by H. Ernst [1], which considers that the load can be represented as the product of two functions: the geometry function $G(a/W)$, and deformation function $H(v_{pl}/W)$, as follows:

$$P = G(a/W)\, H\left(v_{pl}/W\right). \qquad \text{Equation 1}$$

For checking the load separation property and also for the experimental evaluation of the η_{pl} factor, which relates J to the work per unit of uncracked ligament area [2], Sharobeam and Landes [3] proposed the S_{ij} parameter. S_{ij} was defined as the ratio between two P vs. v_{pl} records of two specimens of the same material, geometry, and constraint, having different a/W ratios, as follows:

$$S_{ij} = \left.\frac{P(a_i, v_{pl})}{P(a_j, v_{pl})}\right|_{v_{pl}} = \left.\frac{G\left(\frac{a_i}{W}\right)H\left(\frac{v_{pl}}{W}\right)}{G\left(\frac{a_j}{W}\right)H\left(\frac{v_{pl}}{W}\right)}\right|_{v_{pl}} \quad \text{Equation 2}$$

Here, a_i and a_j are the stationary crack lengths of the i and j specimens, respectively, and v_{pl} is the plastic displacement. If the condition of stationary cracks is maintained and the experimental S_{ij} is constant, then $G(a_i/W)/G(a_j/W)$ = constant, the load is separable and S_{ij} depends only on the geometry functions. Therefore, if a set of P vs. v_{pl} records are created for different a_i/W ratios (always in stationary crack condition) and anyone of them is taken as reference (with a given value of a_j/W), the division of the another records by the chosen one will result in a set of parallel straight horizontal lines S_{ij} vs. v_{pl}. Subsequently, a plot of S_{ij} vs. a_i/W (or b_i/W) will provide the functional form of $G(a/W)$ [4]. Sharobeam and Landes [3] suggested that the geometrical function form can be written as a power law function, as follows:

$$S_{ij} = A\left(\frac{b_i}{W}\right)^m, \quad \text{Equation 3}$$

where

$$A = \left(\frac{b_j}{W}\right)^{-m} \quad \text{Equation 4}$$

and b_j = constant for BN specimens. The m exponent is equal to η_{pl}, defined as:

$$m = \eta_{pl} = \frac{b_i}{W}\frac{m(b_i/W)^{m-1}}{(b_i/W)^m} \quad \text{Equation 5}$$

After this investigation for stationary cracks, Sharobeam and Landes [5] extended the methodology and proposed the S_{pb} parameter, which is a particular form of the method applied to PC specimens as the loading ratio between a PC and BN samples. Then, for the same material, geometry, and constraints, the S_{pb} parameter was defined as:

$$S_{pb} = \left.\frac{P_p}{P_b}\right|_{v_{pl}} = \left.\frac{G_p\left(\frac{b_p}{W}\right)H_p\left(\frac{v_{pl}}{W}\right)}{G_b\left(\frac{b_b}{W}\right)H_b\left(\frac{v_{pl}}{W}\right)}\right|_{v_{pl}}, \quad \text{Equation 6}$$

where the subscript p represents the PC specimen and b de BN specimen.

Additionally, Sharobeam and Landes corroborated the separability of load in PC specimens of three different materials in C(T) geometry. As S_{pb} versus b_p/W (on logarithmic coordinates) showed a straight line behavior in the tearing region [5], Equation 6 can be written as:

$$S_{pb} = \frac{G_p\left(\frac{b_p}{W}\right)}{G_b\left(\frac{b_b}{W}\right)} = A\left(\frac{b_p}{W}\right)^m, \qquad \text{Equation 7}$$

where

$$A = \left(\frac{b_b}{W}\right)^{-m} \qquad \text{Equation 8}$$

and b_b = constant.

Up to this point, as proposed by Sharobeam and Landes, the S_{ij} and S_{pb} parameters were only used to verify the load separation property and to estimate the experimental η_{pl} factor both for BN and PC specimens. However, it was not until the proposal of Wainstein et al. [6] that the method was used to estimate the crack length in PC specimens. An alternative and simplified form of the S_{pb} parameter to estimate the crack length was proposed:

$$S_{pb} = \left(\frac{b_p}{b_b}\right)^m \qquad \text{Equation 9}$$

This assumption implies that the power law of the geometry function for BN and PC specimens should have the same m exponent, *i.e.* the same η_{pl} factor. Then, if the exponent m is known, the instantaneous crack length for the whole plastic record can be calculated as:

$$a_p = W - b_p = W - b_b\left(S_{pb}\big|_{v_{pl}}\right)^{1/m} \qquad \text{Equation 10}$$

Commonly, m is determined through three calibration points, two of them corresponding to the initial and the final crack lengths, and a third theoretical calibration point (conventionally at S_{pb} = 1, where a_p and a_b are the same). Then, taking logarithms to Equation 9 and using these three points, m can be calculated through a linear regression.

The simplified form of S_{pb} (Equation 9) has been applied to determine the crack length in different geometries and materials [6–15]. Nevertheless, this S_{pb} application uses a power law expression that corresponds to a condition where η_{pl} is the same for both specimens and constant during the test. When the methodology is applied to geometries where the η_{pl} factor depends on the a/W ratio this condition is not always maintained. In these cases, its application can lead to differences in crack length measurements.

The present work is focused on a theoretical analysis of the S_{pb} parameter applied to different normalized geometries of fracture toughness tests specimens, particularly in those where η_{pl} depends on the a/W ratio (*i.e.* C(T) and SE(T) geometries). Some modifications for improving the accuracy of the S_{pb} methodology for these geometries are proposed and experimental results from C(T) and SE(T) geometries including these modifications are analyzed.

2 Materials and Methods

2.1 *Material*

The experimental tests were performed on a structural ASTM A572 Gr50 steel. The mechanical properties of the material are shown in Table 1.

Table 1 - Mechanical properties of the tested steel.

Material	σ_{YS} [MPa]	σ_{UTS} [MPa]	Elongation at break [%]
ASTM A572 Gr50	407	506	48

2.2 Fracture toughness tests

The fracture toughness tests were performed in three standard geometries: SE(B), C(T), and clamped SE(T). Specimens of C(T) and SE(B) geometries were machined according to the ASTM E1820-18a standard [16]. SE(T) specimens were machined according to the BS 8571 [17] standard. Some specimens were fatigue pre-cracked in three-point bending. The maximum pre-cracking loads were calculated according to the ASTM E1820 standard [16]. Besides, blunt notched specimens having notch-tip diameter of 3.0 mm were also machined for the application of the S_{pb} method. The dimensions of the specimens, the initial crack length to width ratios, and the final crack length (pre-cracked specimens) are shown in Table 2. Integral or attached knife edges were indistinctly used in the BN specimens.

During testing of pre-cracked specimens, the unloading compliance technique was also applied, while monotonic tests were performed for the BN specimens. The specimens were tested at 1 mm/min in displacement rate, in air and at room temperature. Two servo-hydraulic testing machines were used: an MTS Landmark instrumented with a ±100kN load cell for SE(B) and

C(T) specimens, and a more powerful Instron 1332 instrumented with a ±250kN load cell for SE(T) specimens. An MTS model 632.03F-31 fracture extensometer (6 mm gage length and 12 mm displacement range) was used in all tests.

Table 2 – Geometry, nomenclature, dimensions (in mm) and *a/W* ratios of the test specimens.

Geometry	Specimen	W	B	a_0	a/W	a_f
SE(B)	PC05	50.00	25.04	25.54	0.51	30.10
	BN05	50.01	25.01	25.26	0.51	-
	BN06	50.00	25.02	30.13	0.60	-
	BN07	50.02	25.02	35.13	0.70	-
C(T)	PC04	40.14	20.03	18.67	0.47	22.98
	PC05	40.02	20.01	21.47	0.54	24.93
	PC07	40.05	20.03	28.26	0.71	31.09
	BN05	40.03	20.02	19.51	0.49	-
	BN06	40.04	20.01	24.14	0.60	-
	BN07	40.01	20.03	28.19	0.70	-
	BN08	40.02	20.02	31.87	0.79	-
SE(T)	PC05	10.02	20.01	5.22	0.52	6.71
	BN05	10.00	20.01	5.25	0.53	-
	BN06	10.01	20.02	6.00	0.60	-
	BN07a	10.03	20.01	6.93	0.69	-
	BN07b	10.02	20.00	7.32	0.73	-

2.3 Crack length measurements

For the instantaneous crack length estimation, both the S_{pb} method and the unloading compliance technique were used. For the SE(B) and C(T) geometries the compliance solutions in annexes A1.4.3, and A2.4.3 of the ASTM E1820 18-a standard [16] were used. For SE(T) geometry, the compliance solutions developed by Cravero and Ruggieri [18] were employed, as recommended in BS 8571 standard [17]. The initial and final physical crack lengths were measured in the fracture surface through the methodology presented in ISO 12135:2016(E) [19] standard.

2.4 The η_{pl} factors

The η_{pl} factors for SE(B) and C(T) geometries were obtained from the annexes A1.4.2.1 and A2.4.2.1 of the ASTM E1820 18-a standard, respectively. All these η_{pl} solutions are based on the load-line displacement (LLD). The η_{pl} factor of SE(T) geometry, based in this case on crack-mouth opening displacement, was obtained from the BS 8571 standard. Additionally, experimental η_{pl} factors were evaluated through the S_{pb} method [10]. Figure 1 shows the standard η_{pl} factor values over the allowed a/W ranges of applicability for these three geometries. As can be seen, η_{pl} remains constant (1.9) over the whole a/W range only for SE(B) geometry.

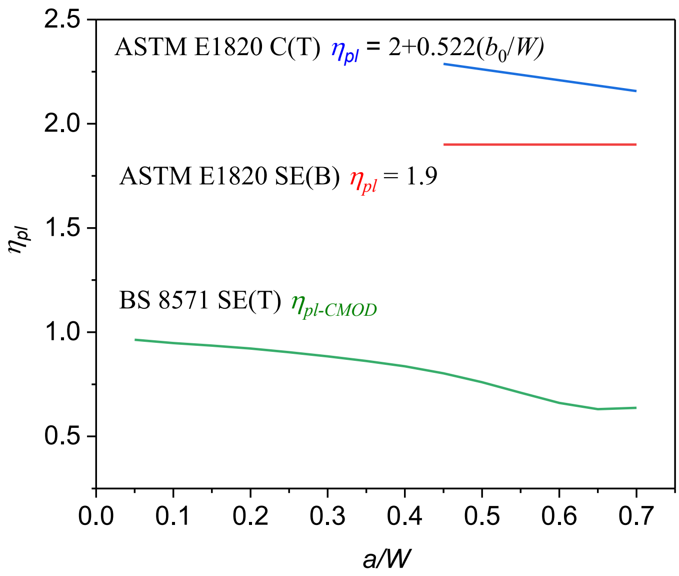

Figure 1. Variation of the η_{pl} factor with a/W for different geometries.

3 Results and Discussion

3.1 Theoretical Analysis

A theoretical analysis of the load separation method applied to the S_{pb} parameter is presented in this section. The S_{pb} parameter, used to estimate the crack extension, has been traditionally applied through Equation 9, which was proposed by Wainstein *et al*. in [6] and represents a simplified expression of Equation 7. Although Sharobeam and Landes have suggested this particular condition [5], they did not represent it as a mathematical expression, due perhaps to its limited validity.

The S_{pb} method requires the load separability existence, but Equation 9 requires additionally that the exponent m does not depend on a/W. The power-law model was proposed for the situation in which η_{pl} is independent on a/W, as occurs for SE(B) geometry. Instead, in geometries where η_{pl} depends on a/W (as in C(T) and SE(T) ones), this model is not strictly valid out of the condition $b_p = b_b$. If Equation 9 is applied to the aforementioned geometries out of this condition two uncertainties are introduced: one caused by the difference between the η_{pl} corresponding to b_p and b_b, and the another one caused by the variation of η_{pl} due to the stable crack growth in the pre-cracked specimen. On the other hand, if Equation 7 is used considering a constant η_{pl} for the PC specimen, only uncertainties due to the variation of η_{pl} by stable crack growth are introduced in the S_{pb} methodology because the η_{pl} factor corresponding to b_b is implicit in the A constant.

The estimation of the m exponent values can be done experimentally, although according to Sharobeam *et al*. [20], the experimental η_{pl} should be preferred only if the calculated value seems not to be appropriate. This is not the state-of-the-art in all cases, because the η_{pl} factors for normalized C(T) and SE(B) geometries are well defined in the standards and these solutions are widely accepted. On the other hand, that seems not to be yet the case for SE(T) geometries. The standard for the fracture toughness evaluation based on this geometry was introduced in 2014 and is still under development [21,22]. As well as, the theoretical η_{pl} for this geometry were also recently proposed and several solutions are now available [23,24]. When Equation 9 is applied to geometries other than SE(B), the m value obtained experimentally cannot be related to a specific η_{pl} because it involves different a/W values corresponding to the BN specimen and the PC one (which varies with Δa). In order to estimate these differences, theoretical S_{pb} vs. a_p/W (b_p/W) curves were created by changing the b_p/W ratio over the whole range allowed by the standards with the η_{pl} factors calculated from the standards solutions. Four theoretical cases were considered:

I. Based on the more general expression of the load separation method (Equation 7), as the a_p/W ratio changes by stable crack growth the respective η_{pl} factor is modified. On the other hand, the a_b/W ratio and its corresponding η_{pl} factor are constant. This case was assumed as the most representative of the experimental conditions and taken as reference.

II. Based on the simplified S_{pb} form (Equation 9), as the a_p/W ratio changes by crack growth the respective η_{pl} factor is modified. The η_{pl} factor for the BN specimen is not explicit in this case, which evaluates the differences introduced by using different a/W ratios in PC and BN specimens.

III. Based on the simplified S_{pb} form (Equation 9), the η_{pl} factor was evaluated only for a_0/W and then maintained constant, which is the direct application of the proposed S_{pb} methodology. This case was useful to assess differences due to the variation of the a_p/W ratio in the simplified form.

IV. Based on the more general expression of the load separation method (Equation 7), the η_{pl} factor related to the PC specimen was evaluated only for a_0/W and then maintained constant. This situation was useful to evaluate the differences introduced by the variation of a_p/W when the general expression is applied.

As SE(B) specimens will feature the same results whenever Equation 7 or 9 is used and no differences will be introduced by stable crack growth the four proposed cases were analyzed only on C(T) and SE(T) geometries, in which η_{pl} depends on a/W.

With the purpose to calculate the theoretical differences between the case I and the cases II, III and IV, the percent difference in the S_{pb} parameter among each case was calculated as:

$$Diff.\% = \frac{S_{pb}^{I} - S_{pb}^{II,III\ or\ IV}}{S_{pb}^{I}} * 100 \qquad \text{Equation 11}$$

Figure 2 shows S_{pb} vs. a_p/W curves (in a log/log scale) and *Diff.%* vs. a_p/W curves for several b_b/W used as reference calculated according to the I and II cases for C(T) and SE(T) geometries. These curves can be also interpreted as the S_{pb} values for different a_p/W and a_b/W ratios. Please note that as the crack length increases, a given point in the theoretical curves in Figures 2, 3, and 4 moves from the right to the left.

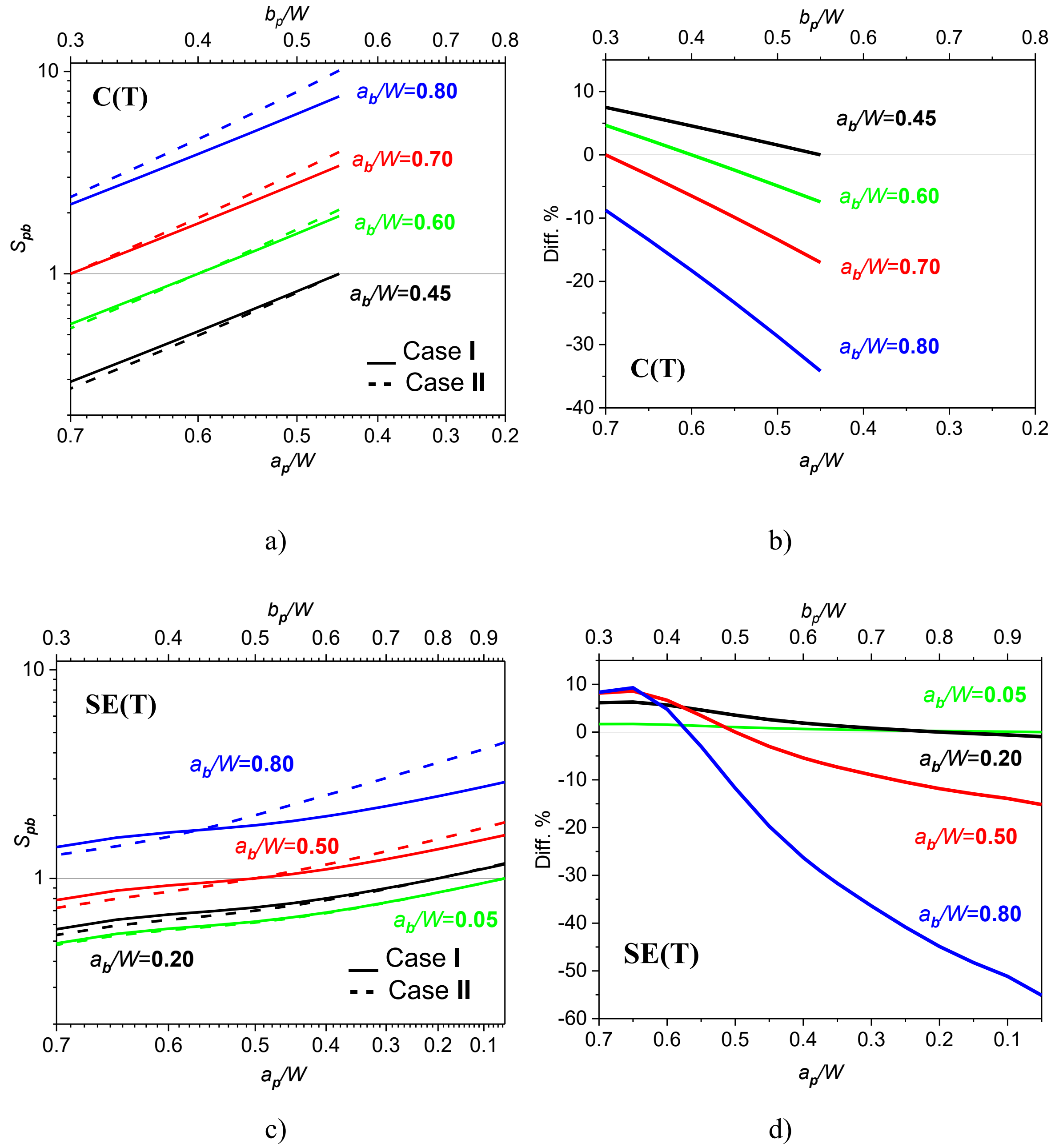

Figure 2. Theoretical S_{pb} vs. a_p/W curves for cases I and II: a) for C(T) geometry, and c) for SE(T) geometry. *Diff%* vs. a_p/W curves for the same cases: b) for C(T) geometry, and d) for SE(T) geometry.

The behavior shown in Figure 2a and 2c by the S_{pb} curves for the case I deserves an observation: although for the C(T) geometry the η_{pl} factor depends on a/W, this does not seem to have much effect on the S_{pb} values. As can be seen, these curves are almost straight in a log-log plane and adherent to a power-law function, which is the geometry function proposed by Sharobeam and

Landes. On the other hand, as the S_{pb} curves for the SE(T) geometry are far from straight in a log-log plane, the use of a power law as geometry function can lead to some additional differences.

As can be seen in from Figure 2b and 2d the highest differences between cases I and II are present when opposite a/W ratios are used in PC and BN specimens. They can be as large as -35% for pre-cracked C(T) specimens having a_p/W = 0.45 and blunt-notch C(T) specimens having a_b/W = 0.80 (blue curve in Figure 2b), and -55% for SE(T) specimens having a_p/W = 0.05 and a_b/W = 0.80 (blue curve in Figure 2d). These configurations for BN specimens are very usual in experimental tests, particularly in SE(B) and C(T) geometries [14,25].

Focusing on the difference introduced by stable crack growth in the range allowed by the standards when simplified expression is used (*i.e.* Δa_{max}= 0.25b_0 for ASTM E1820 and 0.20b_0 for BS 8571) curves with different a_0/W ratios were plotted for C(T) and SE(T) geometries based on the case III. The differences related to Δa in Figure 3 can be interpreted as the variation of S_{pb} with the stable crack growth when fixing a η_{pl} factor for some a_0/W value.

Figure 3 shows theoretical S_{pb} vs. a_p/W curves for C(T) and SE(T) geometries according to the cases I and III, as well as *Diff%* vs. a_p/W curves for several a_0/W ratios. Focusing on the analysis of the differences introduced by Δa, only the dot curves can be discussed, because they begin at the S_{pb}=1 condition and, consequently, no differences related to the Case II are present in this situation. When this condition is analyzed for C(T) geometry (a_0/W = 0.45), it can be seen that the difference at Δa_{max} is close to 7% (Figure 3b). On the other hand, for SE(T) geometry, S_{pb}=1 is attained for two a_0/W ratios (a_0/W = 0.05 and 0.5). Among them, the maximum difference is reached for a_0/W = 0.5 (Figure 3d) and is lower than 10%.

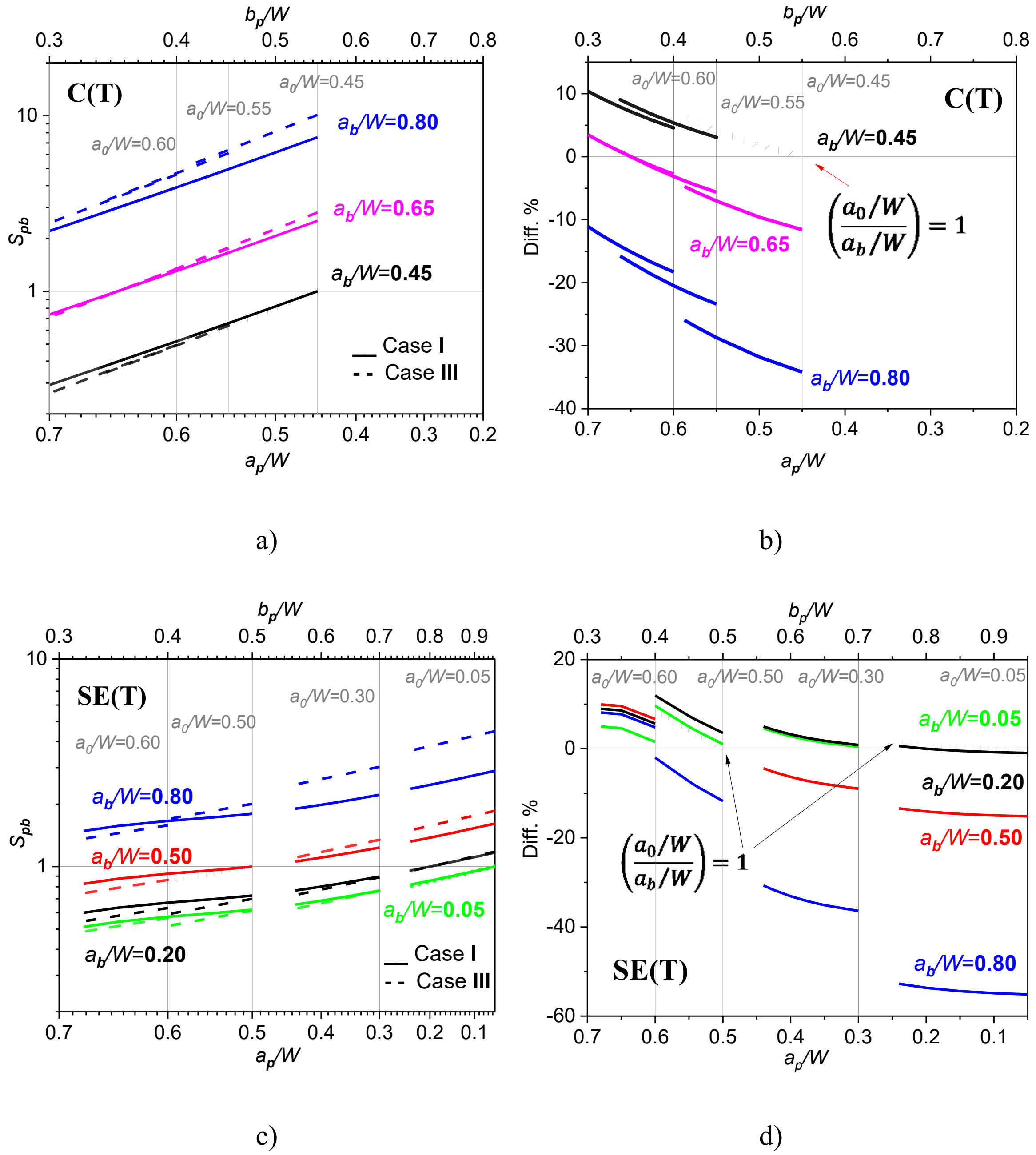

Figure 3. Theoretical S_{pb} vs. a_p/W curves for cases I and III: a) for C(T) geometry, and c) for SE(T) geometry. *Diff%* vs. a_p/W curves for the same cases: b) for C(T) geometry, and d) for SE(T) geometry.

Figure 4 shows theoretical S_{pb} vs. a_p/W curves for C(T) and SE(T) geometries according to the cases I and IV, as well as *Diff%* vs. a_p/W curves for several b_0/W ratios. Regarding the analysis based on the case IV, the S_{pb} *vs.* a_p/W curves (Figure 4a and 4c) shows that the use of any a_b/W ratio as reference leads to similar results. These curves are coincident for every a_0/W ratio

(Figure 4b and 4d). This behavior confirmed that if the general expression for S_{pb} is used instead of the simplified form; the differences will be only due to the b_0/W variation. In other words, the only source of differences will the stable crack growth.

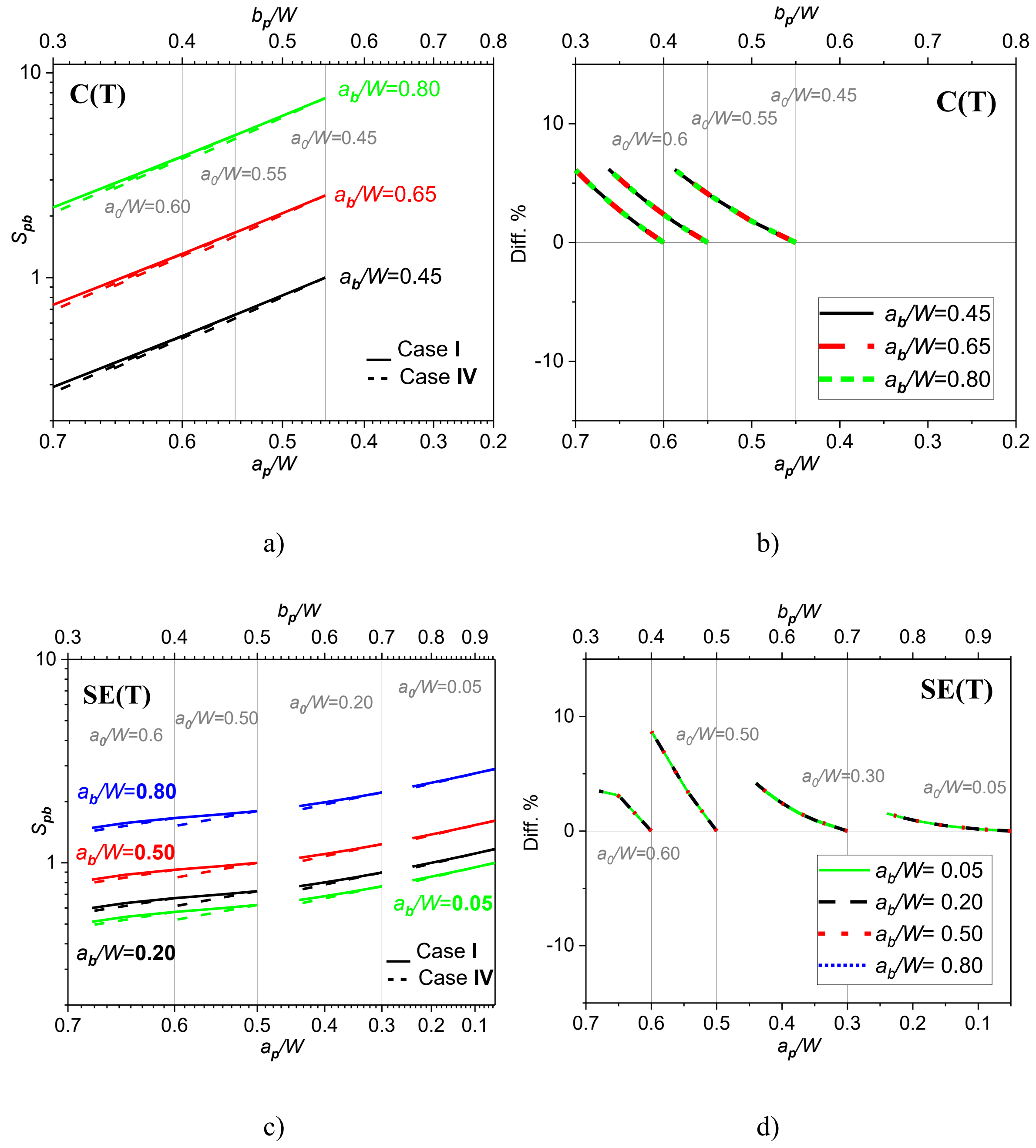

Figure 4. Theoretical S_{pb} vs. a_p/W curves for cases I and IV: a) for C(T) geometry, and c) for SE(T) geometry. *Diff%* vs. a_p/W curves for the same cases: b) for C(T) geometry, and d) for SE(T) geometry.

Besides, the results showed that for C(T) geometry (Figure 4b), the maximum difference (around 6 to 7%) is attained at Δa_{max} and is independent of the chosen a_0/W ratio. On the other hand, for the SE(T) geometry, the results indicate that the differences evaluated at Δa_{max} (Figure 4d) depend on the chosen a_0/W ratio. As can be seen, the maximum differences were attained when a_0/W=0.5.

3.2 Experimental results

3.2.1 Plastic displacement records

Typical P vs. LLD_{pl} records for SE(B) and C(T) geometries are shown in Figure 5. For the sake of clarity unloading and reloading sequences for compliance measurements were removed.

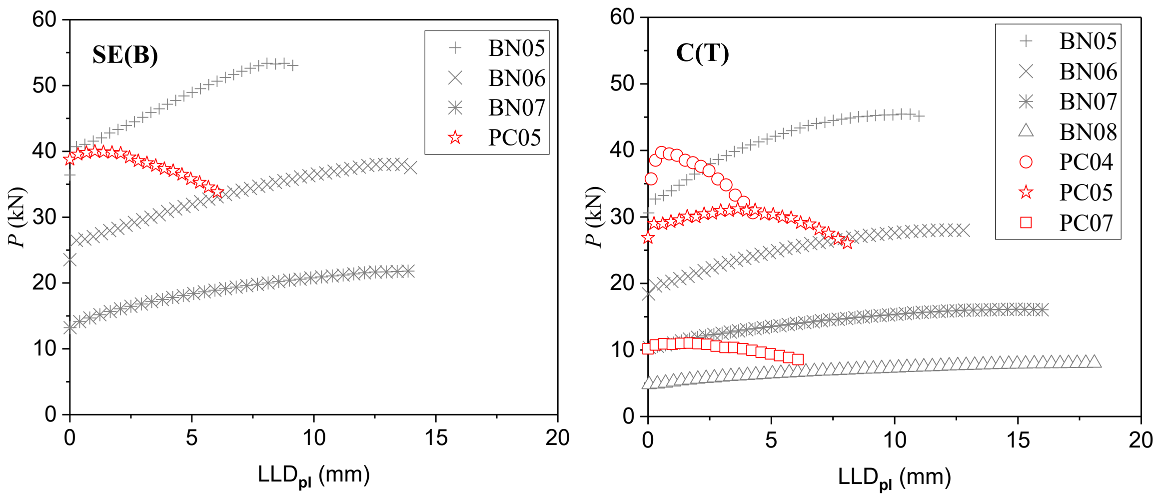

a) b)

Figure 5. Experimental P *vs.* LLD_{pl} records for several PC and BN specimens: a) SE(B) geometry, and b) C(T) geometry.

Along the tests of SE(T) geometry, evidence of plastic deformation far from the uncracked ligament were clearly present, as shown by the deformations bands in Figure 6. As in the presence of plasticity far from the uncracked ligament the validity of η_{pl} cannot be assured [2], the application of the S_{pb} methodology based on P-LLD records in SE(T) specimens is not recommended. Based on that it was decided to apply the S_{pb} methodology in this geometry based on P-CMOD records. Even if the CMOD evaluation (which requires the use of an extensometer) eliminates one of the main advantages to the S_{pb} method, it can still be competitive because the monotonic test of only two specimens is required, which continued to be attractive if compared to UC (which requires the use of an extensometer and the accurate control of unloading and reloading sequences) or multi-specimen methodologies (which requires at least 6 identical specimens). Typical P *vs*. $CMOD_{pl}$ records for SE(T) specimens are shown in Figure 7. Once again, unloading and reloading sequences were removed from these records.

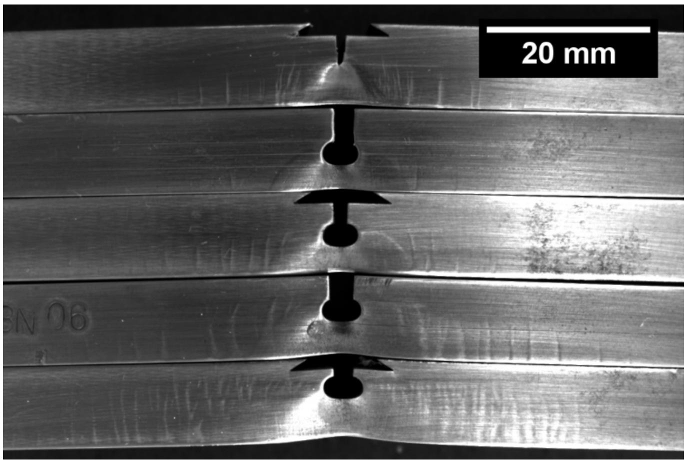

Figure 6. SE(T) specimens show deformations bands outside the uncracked ligament.

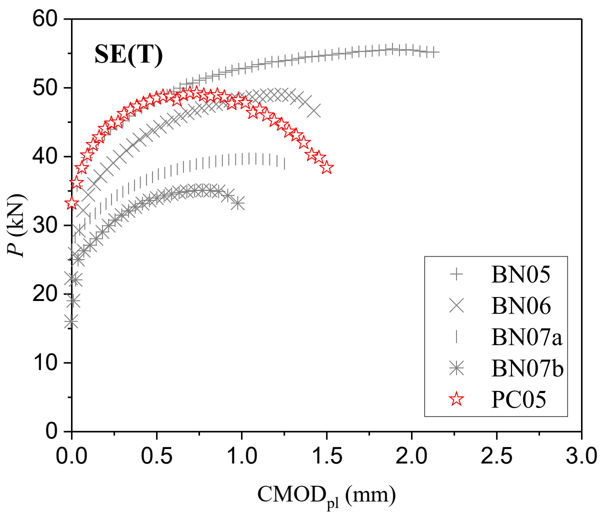

Figure 7. Experimental P *vs.* $CMOD_{pl}$ records of several PC and BN specimens in SE(T) geometry.

Focusing on the experimental records shown in Figure 5 and Figure 7, it is possible to see that for SE(B) and C(T) specimens the amount of plastic displacements till the maximum loading increases with the *a/W* ratios of BN specimens. On the other hand, the plastic displacement till the maximum loading decreases with the increase in *a/W* for the BN specimens of SE(T) geometry. As the applicability of the S_{pb} methodology requires higher plastic displacement of the BN specimen than the PC ones [8], the use of SE(T) BN specimens having higher *a/W* ratios was a limitation in this case and, as a result, some configurations evaluated in the theoretical analysis were not experimentally feasible. In practice, when the S_{pb} method is applied in SE(T) geometry it would be more convenient to use small a_b/W ratios as reference.

3.2.2 Experimental η_{pl} factors

When possible, experimental η_{pl} factors based on the S_{pb} method for the three geometries were evaluated. For these calculations, results from one PC specimen with results from several BN specimen were combined. The experimental and theoretical η_{pl} factors (for a_0 and a_f when applicable), as well as the difference between them, are shown in Table 3. As can be seen, the experimental and theoretical η_{pl} factors are almost coincident for the SE(B) geometry. For the C(T) geometry the differences between experimental and theoretical η_{pl} values are higher than for SE(B) geometry (between 4% and 16%), but these differences are systematically lower for longer crack sizes (a_f). On the other hand, differences between experimental and theoretical η_{pl} for SE(T) geometry were the biggest ones. For this geometry, the experimental η_{pl} factor is almost one, but caution is needed here, because this result was taken from only one valid test. Additional experimental work needs to be done here to elucidate this point.

Table 3 - Experimental η_{pl} factors estimated through the S_{pb} method.

PC	BN	Experimental η_{pl}	Theoretical η_{pl}		|Difference| (%)	
			a_0	a_f	a_0	a_f
SE(B) PC05	BN05	1.91	1.9		0.53	
	BN06	1.94			2.11	
	BN07	1.92			1.05	
C(T) PC04	BN05	2.12	2.28	2.22	7.07	4.73

	BN06	2.12			6.95	4.60
	BN07	2.03			10.93	8.69
	BN08	2.01			11.98	9.76
C(T) PC05	BN05	1.88	2.24	2.20	16.07	14.55
	BN06	2.09			6.70	5.00
	BN07	2.08			7.14	5.45
	BN08	2.04			8.93	7.27
C(T) PC07	BN05	2.03	2.15	2.12	5.83	4.19
	BN06	2.01			6.79	5.16
	BN07	1.97			8.50	6.90
	BN08	1.90			11.67	10.13
SE(T) PC05	BN05	0.98	0.74	0.63	24.49	35.71

3.2.3 Crack extension

Several crack extensions along the tests were estimated by the S_{pb} methodology according to three different situations:

a) According to the Case III using Equation 10 with the experimental η_{pl} factors of Table 4 (that is, the simplified S_{pb} methodology);

b) According to the Case IV using the general expression for S_{pb} with η_{pl} factors from the standards. For that, it was necessary to rearrange Equation 7 as follows:

$$a_p = W - b_p = W\left(S_{pb}\left(\frac{b_b}{W}\right)^{\eta_{pl}^{BN}}\right)^{1/\eta_{pl}^{PC}} \qquad \text{Equation 12}$$

c) Since the instantaneous crack length calculated by S_{pb} depends on the initial and final physical crack lengths, the direct application of Case I was not possible. Thus, in one attempt to simulate this situation an iterative procedure for the solution of Equation 12 was proposed based in the following steps:

   1) At the first step all the crack lengths were calculated through the Equation 12 using η_{pl} evaluated at a_0;

   2) Corrected a_i crack lengths were calculated by the re-application of Equation 12, in this case with η_{pl} from the previous step crack lengths;

3) The second step was repeated till a certain convergence in physical final crack length (a_f) was attained.

Finally, three kinds crack length vs. displacement curves were obtained according to the three situations above. The first kind corresponds to the a) situation, defined as S_{pb}S; the second kind of curves corresponds to the b) situation and were defined as S_{pb}*; and the curves corresponding to the c) situation, which were defined as S_{pb}*corr. All these results were compared to those from the unloading compliance technique.

3.2.3.1 SE(B) geometry

Experimental a vs. LLD_{pl} curves for the specimens of SE(B) geometry are shown in Figure 8. As the η_{pl} factor is independent of a/W ratio in this geometry, only S_{pb}S results were plotted. As expected, the crack extension values estimated through the S_{pb} method and those from UC are in good agreement.

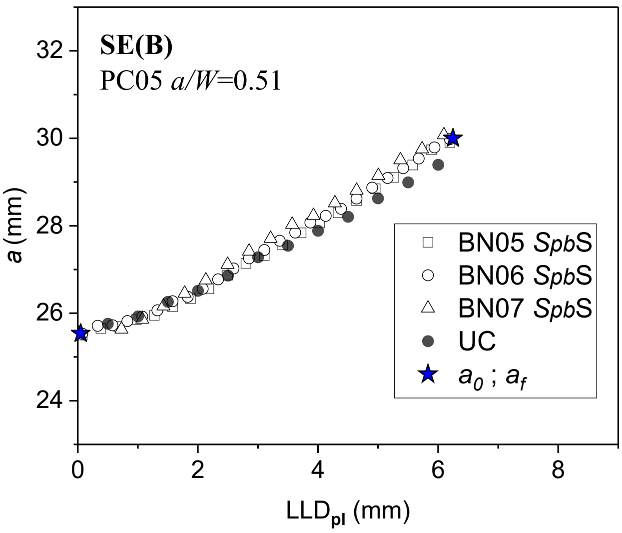

Figure 8. Experimental a vs. LLD_{pl} curves obtained through UC and the simplified S_{pb} equation for SE(B) geometry.

3.2.3.2 C(T) geometry

Figure 9a, Figure 10a, and Figure 11a show the experimental a *vs.* LLD_{pl} curves for C(T) specimens with a_p/W = 0.45, 0.55 and 0.70, respectively (using the BN07 as reference). As can be seen, the results obtained through S_{pb}*corr are in good agreement to the UC technique. Additionally, Figure 9b, Figure 10b, and Figure 11b show a comparison of crack extensions from the UC technique and the three analyzed S_{pb} situations. The proposed methodology lead to good results for pre-cracked C(T) specimens having *a/W* from 0.45 to 0.70 (the whole range allowed by the ASTM standards), showing the best results for *a/W* between 0.45 and 0.55, the most widely used experimental ratios.

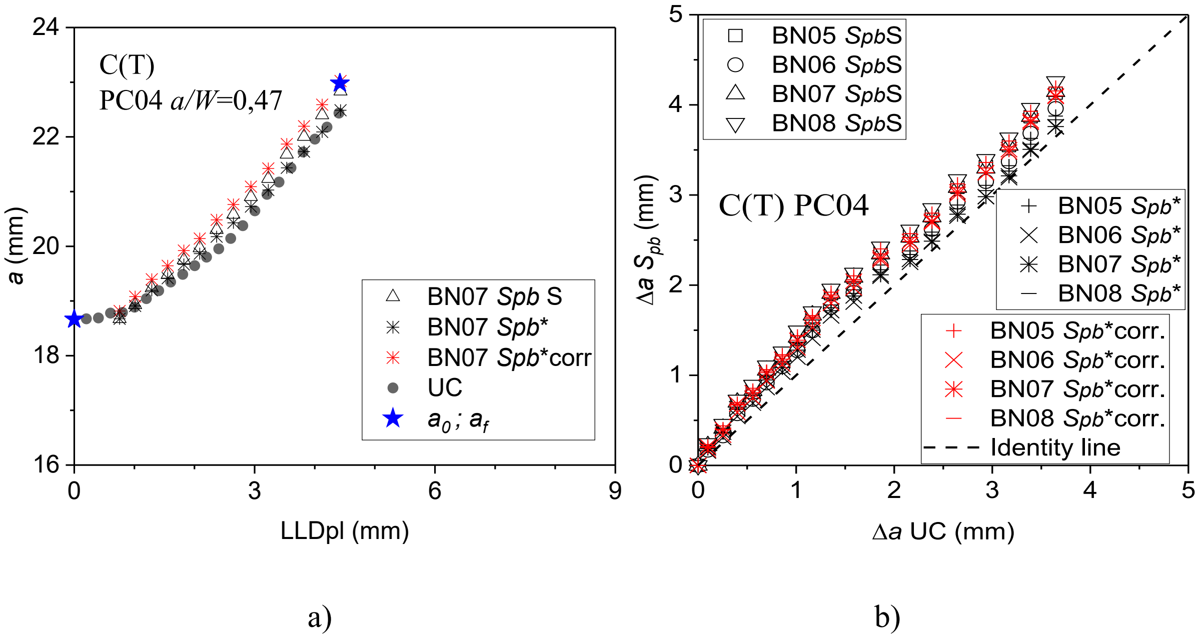

Figure 9. C(T) PC04 specimen (*a/W* = 0.45): a) Comparison of crack extensions obtained through UC and S_{pb} method, and b) Δa of unloading compliance against Δa of S_{pb}S, S_{pb}* and S_{pb}*corr.

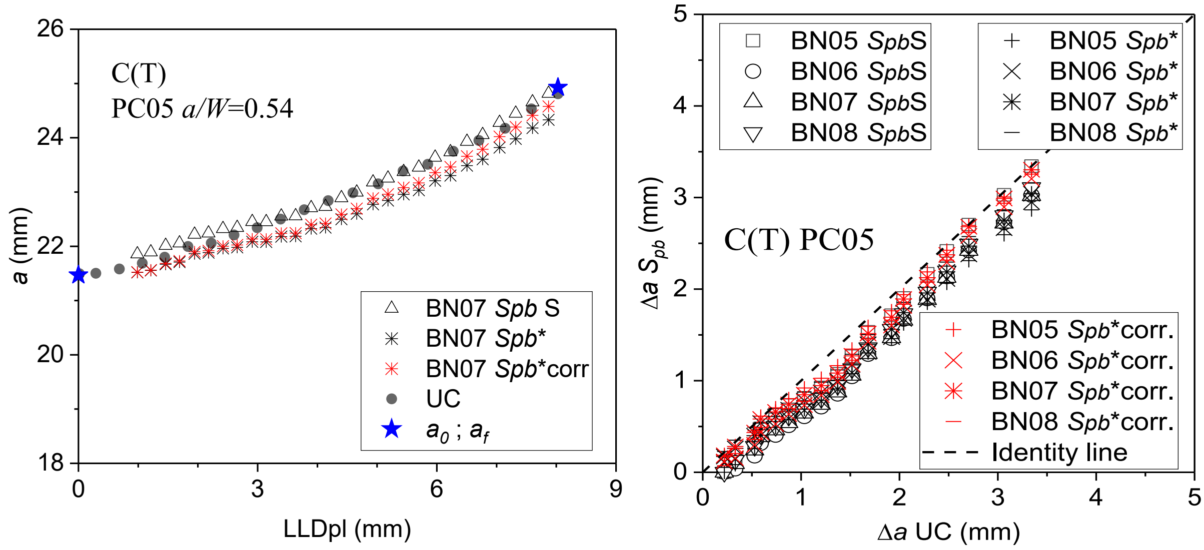

a) b)

Figure 10. C(T) PC05 specimen (a/W = 0.54): a) Comparison of crack extensions obtained through UC and S_{pb} method, and b) Δa of unloading compliance against Δa of S_{pb}S, S_{pb}* and S_{pb}*corr.

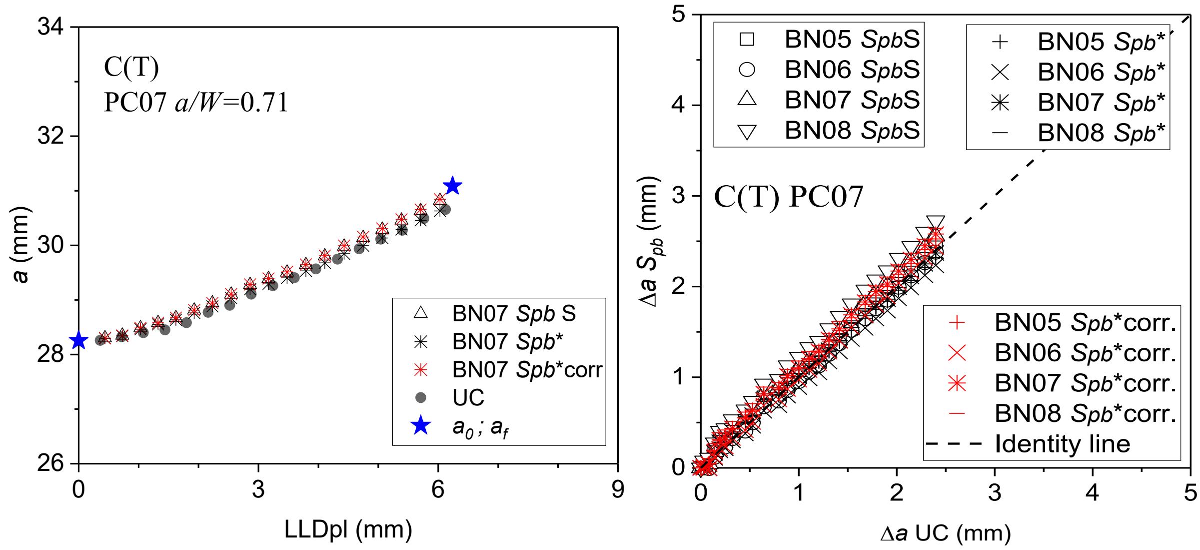

a) b)

Figure 11. C(T) PC07 specimen (a/W = 0.71): a) Comparison of crack extensions obtained through UC and S_{pb} method, and b) Δa of unloading compliance against Δa of S_{pb}S, S_{pb}* and S_{pb}*corr.

3.2.3.3 SE(T) geometry

Focusing on the applicability of the S_{pb} method to SE(T) geometry, it is interesting to note that, as can be seen in Figure 7, for BN specimens the higher the *a/W* ratio, the lower the useful plastic displacement. As a result, for the application of S_{pb} method, BN specimens need to have the same or lower *a/W* ratios than the PC specimen, opposite to the SE(B) and C(T) geometries. Because of that, only the BN specimen with $a_b/W \approx 0.5$ can be used in the experimental estimation of instantaneous crack size. Additionally, even though the theoretical analysis showed that PC specimens having lower *a/W* ratios could improve the sensitivity of the methodology (Figure 4d), additional tests could not be performed to evaluate this point.

Regarding the crack extension results, the use of the S_{pb}S shows curves that almost collapsed to one single curve with the UC technique. On the other hand, the results obtained by using S_{pb}* and S_{pb}*corr were not the expected ones. As can be seen (Figure 12), the two proposals overestimated the crack length for larger plastic displacements, S_{pb}*corr being the less accurate. As a result, the situation a) featured best results than the iterative process for this geometry.

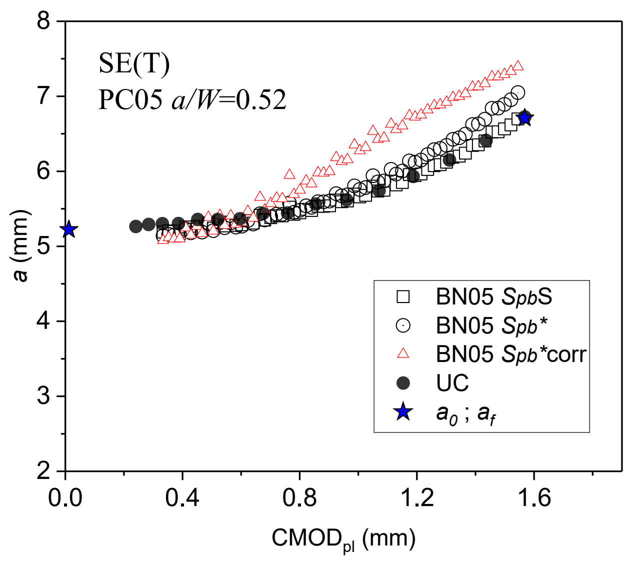

a)

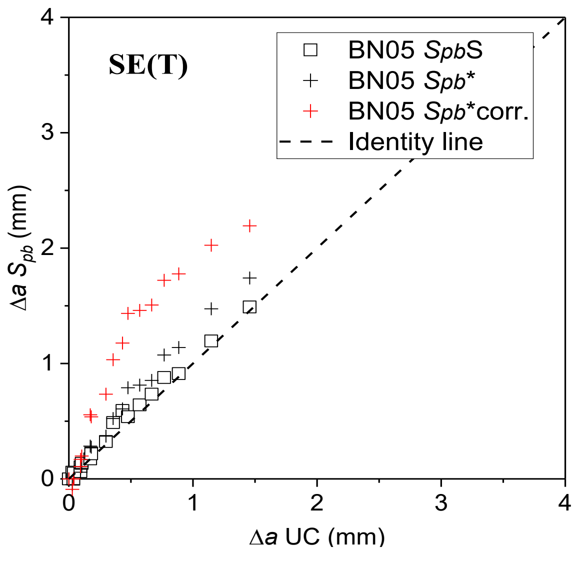

b)

Figure 12. a) Comparison of crack extensions obtained through UC and S_{pb} method, for SE(T) geometry and b) Δa of unloading compliance against Δa of S_{pb}S, S_{pb}* and S_{pb}*corr.

3.2.4 Predicted and physical crack extensions

Regarding to the physical crack extension Δa_p, Table 4 present Δa_p values against the predicted crack extensions estimated through the UC and S_{pb} method (S_{pb}S, S_{pb}^*, S_{pb}^*corr). These results showed that for SE(B) geometry the two used methods lead to results within the limit of the standards. On the other hand, for C(T) geometry the S_{pb}*corr gave better results than S_{pb}* and S_{pb}S in almost all cases. Thus, more accurate results can be obtained when the iterative process is used. Finally, for SE(T) geometry the proposed modifications to the methodology were not useful for improving the accuracy of the $\Delta a_{predicted}$ and all the results fallen out of the limit allowed by the standards.

Table 4. Predicted and physical crack extensions comparisons among UC and S_{pb} methods.

Geometry	PC	Δa_p (mm)	BN	$\Delta a_{predicted}$ (mm)				*Diff%* with Δa_p			
				UC	S_{pb}S	S_{pb}*	S_{pb}*corr	UC	S_{pb}S	S_{pb}*	S_{pb}*corr
SE(B)	PC05	4.56	BN05	3.97	4.54	-	-	12.93	0.44	-	-
			BN06		4.64	-	-		-1.75	-	-
			BN07		4.66	-	-		-2.19	-	-
C(T)	PC04	4.31	BN05	3.77	4.30	4.03	4.37	12.61	0.42	6.53	-1.26
			BN06		4.17	3.96	4.32		3.26	8.24	-0.07
			BN07		4.32	3.92	4.28		-0.18	9.10	0.82
			BN08		4.45	4.01	4.35		-3.19	7.05	-0.74
	PC05	3.46	BN05	3.34	3.38	2.90	3.23	3.47	2.31	<u>16.18</u>	6.64
			BN06		3.07	2.95	3.22		11.27	14.74	6.94
			BN07		3.04	3.01	3.27		12.13	13.00	5.50
			BN08		3.11	3.07	3.26		10.12	11.27	5.80
	PC07	2.83	BN05	2.50	2.57	2.44	2.65	11.62	9.03	13.90	6.25
			BN06		2.51	2.36	2.57		11.14	<u>16.56</u>	9.12
			BN07		2.69	2.50	2.72		4.92	11.80	3.94
			BN08		2.93	2.61	2.84		-3.38	7.93	-0.19
SE(T)	PC05	1.49	BN05	1.46	1.51	1.87	2.24	2.01	-1.34	<u>-25.50</u>	<u>-50.37</u>

Note: underlined numbers are out of the $0.15\Delta a_p$ allowed by the standards.

4 Concluding remarks

The analysis of the theoretical and experimental results suggested that:

- For the studied geometries where η_{pl} depends on a/W the theoretical analysis showed that the maximum differences in the simplified form of the S_{pb} are present when the same η_{pl} for the PC and BN specimens is considered (Case II). This difference is higher than the obtained when assuming η_{pl} as a constant (Case III).
- For geometries where η_{pl} depends on a/W the theoretical analysis showed that higher accurate crack length estimates can be made through the more general expression of S_{pb} (Equation 7) in addition to the η_{pl} given by the standards. On the other hand, by using this approach estimates of the m parameter are not necessary.
- Due to plastic deformation outside the remaining ligament in specimens of SE(T) geometry, it is recommendable to use CMOD instead LLD displacements when using the S_{pb} methodology. For this specific geometry (W/B = 0.5) and material, the experimental results showed that the η_{pl} based on CMOD displacements is near the unit.
- The use larger a/W ratios on BN than in PC specimens is not recommended for SE(T) geometry, because attaining the required plastic displacements of BN specimens for the application of the S_{pb} method could be not possible.
- The experimental results of crack extension (Δa) for the C(T) geometry estimated through the proposed iterative process were in close agreement with those obtained by the UC technique and fit in both cases the limit imposed by the standards. These results were in best agreement than those obtained through the simplified form of S_{pb} in most of the cases.
- For the SE(T) geometry, the results obtained through the simplified form of S_{pb} were better than those obtained by the proposed modifications, based on the η_{pl} factors provided by the literature. Additional research is needed for a better understanding of this behavior.

Acknowledgments

To Jorge A. C. Cohn and João T. O. de Menezes for your invaluable contribution to the experimental tests. To the LaH2S Laboratory of the Brazilian National Institute of Technology (INT) for some laboratorial facilities. This study was partially financed by the Brazilian Coordenação de Aperfeiçoamento de Pessoal de Nível Superior (CAPES) Finance Code 001.

References

[1] Ernst H, Paris P, Landes J. Estimations on J-Integral and Tearing Modulus T from a Single Specimen Test Record. Fract. Mech., West Conshohocken, PA: ASTM International; 1981, p. 476–502. https://doi.org/10.1520/STP28814S.

[2] Paris PC, Ernst H, Turner CE. A J-Integral Approach to Development of η-Factors. Fract. Mech., West Conshohocken: ASTM International; 1980, p. 338–51. https://doi.org/10.1520/STP36979S.

[3] Sharobeam MH, Landes JD. The load separation criterion and methodology in ductile fracture mechanics. Int J Fract 1991;47:81–104. https://doi.org/10.1007/BF00032571.

[4] Landes JD, Zhou Z. Application of load separation and normalization methods for polycarbonate materials. Int J Fract 1993;63:383–93. https://doi.org/10.1007/BF00013045.

[5] Sharobeam MH, Landes JD. The load separation and ηpl development in precracked specimen test records. Int J Fract 1993;59:213–26. https://doi.org/10.1007/BF02555184.

[6] Wainstein J, de Vedia LA, Cassanelli AN. A study to estimate crack length using the separability parameter Spb in steels. Eng Fract Mech 2003;70:2489–96. https://doi.org/10.1016/S0013-7944(02)00288-6.

[7] Shi K, Cai L-X, Bao C, Yao Y. Dimensionless load separation theory using SE(B) specimen and Software development. TELKOMNIKA Indones J Electr Eng 2012;10:2261–6. https://doi.org/10.11591/telkomnika.v10i8.1694.

[8] Wainstein J, Perez Ipiña JE. Load-Separation Method, Spb , Used to Estimate Crack Extension for J-R Curves, Modified for Geometric Variations in Blunt-Notched Remaining Ligament. J Test Eval 2017;45:20160027. https://doi.org/10.1520/JTE20160027.

[9] Wainstein J, Perez Ipiña JE. The Spb method used to estimate crack extension for coiled tubings fracture toughness tests. Eng Fract Mech 2017;178:362–74. https://doi.org/10.1016/j.engfracmech.2017.03.014.

[10] Wainstein J, Cocco R, de Vedia L, Cassanelli A. Influence of the Calibration Points on the Spb Parameter Behavior. J Test Eval 2006;35:1–6.

https://doi.org/10.1520/jte100131.

[11] Wainstein J, Fasce LA, Cassanelli A, Frontini PM. High rate toughness of ductile polymers. Eng Fract Mech 2007;74:2070–83. https://doi.org/10.1016/j.engfracmech.2006.10.001.

[12] Salazar A, Rodríguez J. The use of the load separation parameter Spb method to determine the J-R curves of polypropylenes. Polym Test 2008;27:977–84. https://doi.org/10.1016/j.polymertesting.2008.08.013.

[13] Rodríguez C, Maspoch ML, Belzunce FJ. Fracture characterization of ductile polymers through methods based on load separation. Polym Test 2009;28:204–8. https://doi.org/10.1016/j.polymertesting.2008.12.004.

[14] Frontini PM, Fasce LA, Rueda F. Non linear fracture mechanics of polymers: Load Separation and Normalization methods. Eng Fract Mech 2012;79:389–414. https://doi.org/10.1016/j.engfracmech.2011.11.020.

[15] Gosch A, Arbeiter FJ, Berer M, Pinter G. Comparison of J-integral methods for the characterization of tough polypropylene grades close to the glass transition temperature. Eng Fract Mech 2018;203:2–17. https://doi.org/10.1016/j.engfracmech.2018.06.002.

[16] ASTM E1820-18a. Standard Test Method for Measurement of Fracture Toughness. ASTM Int., West Conshohocken, PA: 2018. https://doi.org/10.1520/E1820-18A.

[17] BS 8571:2018. Method of test for determination of fracture toughness in metallic materials using single edge notched tension (SENT) specimens. BSI Stand Publ 2018.

[18] Cravero S, Ruggieri C. Estimation procedure of J-resistance curves for SE(T) fracture specimens using unloading compliance. Eng Fract Mech 2007;74:2735–57. https://doi.org/10.1016/j.engfracmech.2007.01.012.

[19] ISO 12135. Metallic materials - Unified method of test for the determination of quasistatic fracture toughness. Int. Stand., 2016.

[20] Sharobeam M, Landes J, Herrera R. Development of Eta Factors in Elastic-Plastic Fracture Testing Using a Load Separation Technique. Elastic-Plastic Fract. Test Methods, West Conshohocken, PA: 1991, p. 114–32. https://doi.org/10.1520/STP16850S.

[21] Moore P, Pisarski H. SENT testing standard BS 8571 and its ongoing development. Int J Press Vessel Pip 2017;156:2–7. https://doi.org/10.1016/j.ijpvp.2017.05.011.

[22] Zhu X-K. Progress in development of fracture toughness test methods for SENT specimens. Int J Press Vessel Pip 2017;156:40–58. https://doi.org/10.1016/j.ijpvp.2017.07.004.

[23] Bao C, Cai L. Estimation of the J-resistance curve for Cr2Ni2MoV steel using the modified load separation parameter Spb method. J Zhejiang Univ A 2010;11:782–8. https://doi.org/10.1631/jzus.A1000153.

[24] Menezes JTO de, Ipiña JEP, Castrodeza EM. Normalization method for J-R curve determination using SENT specimens. Eng Fract Mech 2018;199:658–71. https://doi.org/10.1016/j.engfracmech.2018.06.033.

[25] Bassindale C, Wang X, Tyson WR, Xu S. Numerical verification of stress intensity factor solution for clamped single edge notched tension (SENT) specimens. Fatigue Fract Eng Mater Struct 2018;41:494–9. https://doi.org/10.1111/ffe.12700.